

Functional Calcium Release Channel Formed by the Carboxyl-Terminal Portion of Ryanodine Receptor

Manjunatha B. Bhat,* Jiying Zhao,* Hiroshi Takeshima,# and Jianjie Ma*

*Department of Physiology and Biophysics, Case Western Reserve University School of Medicine, Cleveland, Ohio 44106 USA, and

#Department of Pharmacology, Faculty of Medicine, University of Tokyo, Hongo, Bunkyo-ku, Tokyo 113, Japan

ABSTRACT The ryanodine receptor (RyR) is one of the key proteins involved in excitation-contraction (E-C) coupling in skeletal muscle, where it functions as a Ca^{2+} release channel in the sarcoplasmic reticulum (SR) membrane. RyR consists of a single polypeptide of ~560 kDa normally arranged in a homotetrameric structure, which contains a carboxyl (C)-terminal transmembrane domain and a large amino (N)-terminal cytoplasmic domain. To test whether the carboxyl-terminal portion of RyR is sufficient to form a Ca^{2+} release channel, we expressed the full-length (RyR-wt) and C-terminal (RyR-C, ~130 kDa) RyR proteins in a Chinese hamster ovary (CHO) cell line, and measured their Ca^{2+} release channel functions in planar lipid bilayer membranes. The single-channel properties of RyR-wt were found to be similar to those of RyR from skeletal muscle SR. The RyR-C protein forms a cation-selective channel that shares some of the channel properties with RyR-wt, including activation by cytoplasmic Ca^{2+} and regulation by ryanodine. Unlike RyR-wt, which exhibits a linear current-voltage relationship and inactivates at millimolar Ca^{2+} , the channels formed by RyR-C display significant inward rectification and fail to close at high cytoplasmic Ca^{2+} . Our results show that the C-terminal portion of RyR contains structures sufficient to form a functional Ca^{2+} release channel, but the N-terminal portion of RyR also affects the ion-conduction and calcium-dependent regulation of the Ca^{2+} release channel.

INTRODUCTION

In striated muscles, coupling of electrical excitation to Ca^{2+} release and myofilament contraction occurs in the junction between the transverse tubule (TT) and the sarcoplasmic reticulum (SR) membranes. Dihydropyridine receptors (DHPRs) located in the TT membrane and ryanodine receptors (RyRs) located in the terminal cisternae of the SR membrane are the two key proteins involved in this process (Fleischer and Inui, 1989; Rios et al., 1991; McPherson and Campbell, 1993). The DHPR functions as the voltage sensor of the TT membrane (Rios et al., 1992), and the RyR constitutes the pathway of the Ca^{2+} release channel (Smith et al., 1985; Imagawa et al., 1987; Ma et al., 1988; Lai et al., 1988; Sutko and Airey, 1996). RyR is a single polypeptide of ~560 kDa that normally exists in a homotetrameric structure with two functional domains. The carboxyl-terminal hydrophobic domain is predicted to contain the conduction pore of the Ca^{2+} release channel, and a large cytoplasmic domain (foot structure) spans the junctional gap between TT and SR membranes, which presumably transmits the electrical excitation signal in the TT membrane into opening of the Ca^{2+} release channel in the SR membrane (Block et al., 1988; Lai et al., 1989; Wagenknecht et al., 1989; Franzini-Armstrong and Jorgensen, 1994). The pre-

cise nature of the coupling of the electrical signal to the release of Ca^{2+} across the triadic junction in E-C coupling remains one of the important unsolved problems in muscle physiology.

The Ca^{2+} release channel from skeletal muscle is a large conductance pore, with a linear conductance of ~100 pS for Ca^{2+} and ~400 pS for monovalent cations (K, Cs) (Lai et al., 1988; Ma et al., 1988; Smith et al., 1988; Brillantes et al., 1994). The activity of the channel reconstituted into lipid bilayer is controlled by cytoplasmic Ca^{2+} through activation and inactivation mechanisms. Ca^{2+} in the nanomolar to micromolar concentration range activates the channel, whereas in the micromolar to millimolar concentrations it inhibits the channel (Coronado et al., 1994; Ma and Zhao, 1994; Meissner, 1994).

The RyRs of skeletal (Takeshima et al., 1989; Zorzato et al., 1990) and cardiac (Nakai et al., 1990; Otsu et al., 1990) muscle are coded by different genes and share a high degree of sequence identity, especially in the carboxyl-terminal regions, where the two proteins are well conserved in their amino acid sequence (Sorrentino and Volpe, 1993; Takeshima, 1993). This region of the protein contains several putative transmembrane segments (Takeshima et al., 1989; Zorzato et al., 1990) and the binding site(s) for Ca^{2+} and ryanodine (Callaway et al., 1994; Witcher et al., 1994). In this study we tested the hypothesis that the pore-forming region of the Ca^{2+} release channel resides in the carboxyl-terminal portion of the RyR protein. Full-length and truncated forms of the skeletal muscle RyR were expressed in Chinese hamster ovary (CHO) cells, and the Ca^{2+} release channel function of these expressed proteins was measured by using a lipid bilayer reconstitution system. Our data show that the carboxyl-terminal ~20% of the RyR protein

Received for publication 31 December 1996 and in final form 20 May 1997.

Address reprint requests to Dr. Jianjie Ma, Department of Physiology and Biophysics, Case Western Reserve University School of Medicine, 10900 Euclid Avenue, Cleveland, OH 44106. Tel.: 216-368-2684; Fax: 216-368-1693; E-mail: jxm63@po.cwru.edu.

© 1997 by the Biophysical Society

0006-3495/97/09/1329/08 \$2.00

contains structures sufficient to form a functional Ca^{2+} release channel.

MATERIALS AND METHODS

Construction of carboxyl-terminal RyR expression plasmids

The entire sequence of the rabbit skeletal muscle RyR cDNA (15.3 kb, RyR-wt) was cloned into the pRRS11 expression vector; the transcription occurs under the control of the SV40 promoter (Takeshima et al., 1989; Penner et al., 1989). Within the RyR cDNA, there is one restriction site for *SalI* (546) and two sites for *XhoI* (6466 and 12018). A deletion mutant of pRRS11 was generated through digestion with *SalI* and *XhoI* and religation with T4 DNA ligase. This mutant lacked the nucleotide sequence from 546 to 12018, which corresponds to a deletion of amino acids from 183 to 4006, and thus is named pRRS11-RyRC. pRRS3, a subclone of pRRS11, contains the cDNA sequence of the carboxyl-terminal RyR (10650–15230) (Takeshima et al., 1989). A 4.2-kb *BamHI* (10982)-*EcoRV* (15230) fragment from pRRS3 was cloned into pcDNA3 expression vector (Invitrogen), followed by the introduction of a 45-bp oligonucleotide containing the following sequence to generate pDNA3-RyRC:

5'-AGCTTCCACCATGGGACATCACCATCACCA
TCACGTGCCGCGGTG-3'

Cells and RyR-C expression systems

CHO cells were grown on 150-mm cell-culture plates at 37°C and 5% CO_2 in Ham's F-12 medium supplemented with 10% fetal bovine serum, 100 units/ml penicillin, and 100 $\mu\text{g}/\text{ml}$ streptomycin. The expression plasmids were introduced into the cells (70–80% confluent) with an electroporation technique in Dulbecco's phosphate-buffered saline (DPBS) containing no Mg^{2+} and Ca^{2+} . Electroporation was carried out with a Gene Pulser II apparatus (Bio-Rad, Richmond, CA) with voltage set at 400 V and capacitance set at 500 μF (time constant 9–11 ms). To compare the efficiency of transfection, control experiments were carried out, as indicated, using lipofectamine (Gibco BRL)-based transfection. The cells were exposed to growth medium containing G418 (0.5 mg/ml) ~48 h after transfection, and harvested at 90–100% confluency for protein expression assay and functional studies.

Immunoprecipitation and Western blot analysis

Control nontransfected CHO cells and those transfected with various expression plasmids were harvested and washed twice with ice-cold DPBS and lysed with 1 ml of ice-cold modified RIPA buffer (150 mM NaCl, 50 mM Tris-Cl, pH 8.0, 1 mM EGTA, 1% Triton X-100, 0.1% sodium dodecyl sulfate (SDS), 1% sodium deoxycholate) in the presence of protease inhibitors (0.5 mM Pefabloc, 1 μM pepstatin, 1 μM leupeptin, 1 $\mu\text{g}/\text{ml}$ aprotinin, and 1 mM benzamidin). The cell lysate was incubated with 4 μg of anti-rabbit skeletal muscle RyR monoclonal antibody RR2 (Takeshima et al., 1989) at 4°C for ~2 h. The protein-antibody complexes were then precipitated with 25 μl protein A-agarose beads. The beads were washed twice with ice-cold RIPA buffer, and the proteins were solubilized with 25 μl gel sample buffer (200 mM Tris-Cl, pH 6.7, 9% SDS, 6% β -mercaptoethanol, 15% glycerol, 0.01% bromophenol blue) and separated on a 3–12% linear SDS-polyacrylamide gel after the samples were heated at 85°C for 5 min. The proteins were then transferred to a polyvinylidene difluoride membrane and blotted with RR2 monoclonal antibody, and with horseradish peroxidase-linked secondary antibody, using the ECL detection system (Amersham Corp.). The epitope for RR2 monoclonal antibody is known to reside in the carboxyl-terminal 656 amino acid region of the skeletal muscle RyR (Takeshima et al., 1993).

Isolation of microsomal membrane vesicles from CHO cells

Microsomal membrane vesicles were isolated from transfected CHO cells. The cells were homogenized on ice in hypotonic lysis buffer (10 mM HEPES, pH 7.4, 1 mM EDTA) containing protease inhibitors (0.5 mM pefabloc-SC, 1 μM pepstatin, 1 μM leupeptin, 1 $\mu\text{g}/\text{ml}$ aprotinin, and 1 mM benzamidin) with 10 strokes in a tight-fitting Dounce homogenizer, followed by 15 strokes after the addition of an equal volume of sucrose buffer (500 mM sucrose, 10 mM HEPES, pH 7.4, 1 mM EDTA). Microsome vesicles were collected by centrifugation of postnuclear supernatant ($10,000 \times g$, 15 min) at $100,000 \times g$ for 45 min at 4°C. The pellet was resuspended in a buffer containing 250 mM sucrose, 10 mM HEPES (pH 7.2). The membrane vesicles were stored at a protein concentration of 2–6 mg/ml at –75°C until use. Usually, 1–3 μl of microsomal membrane vesicles was used for reconstitution of Ca^{2+} release channels in the lipid bilayer system.

Reconstitution of calcium release channels in lipid bilayer membrane

Lipid bilayer membranes were formed across an aperture of ~200 μm diameter with the Muller-Rudin method with a mixture of phosphatidylethanolamine:phosphatidylserine:cholesterol (6:6:1); the lipids were dissolved in decane at a concentration of 40 mg/ml. Incorporation of the Ca^{2+} release channel in bilayer was achieved by the addition of membrane vesicles containing either the RyR-native, RyR-wt, or RyR-C proteins, to the *cis* solution, under a concentration gradient of 200 mM (*cis*)/50 mM (*trans*) cesium-gluconate. Unless otherwise indicated, symmetrical 200 mM Cs-gluconate was used as a current carrier, with 1 mM ATP present in the *cis* solution. The pH in both *cis* and *trans* solutions was maintained throughout the experiment at 7.4 with 10 mM HEPES-Tris. The free Ca^{2+} concentrations in both solutions were buffered with 1 mM EGTA and measured with a Ca^{2+} -sensitive electrode (Orion, Boston, MA). Identification of the Ca^{2+} release channel was based on the following criteria: 1) large conductance (~400 pS in 200 mM Cs) and fast kinetics of gating; 2) activation by micromolar concentrations of cytoplasmic Ca^{2+} ; and 3) modification of the channel function by 1 μM ryanodine. Orientation of the Ca^{2+} release channel in the lipid bilayer, usually in the *cis*-cytoplasmic *trans*-luminal SR manner, was determined by the sensitivity of the channel to cytoplasmic Ca^{2+} and the asymmetric conduction property of the RyR-C channel. Channels oriented in the opposite direction, which account for less than 10% of the experiments, were not used in the present study.

Analysis of single-channel data

To maintain the stability of the bilayer membrane and the Ca^{2+} release channel activities, designed pulse protocols were used to measure currents through the single Ca^{2+} release channels. The bilayer membrane was kept at a holding potential of 0 mV, and pulsed to different test potentials of 0.5–1-s duration. Single-channel currents were recorded with an Axopatch 200A patch-clamp unit (Axon Instruments, Foster City, CA). Data acquisition and pulse generation were performed with a 486 computer and 1200 Digidata A/D-D/A convertor (Axon Instruments). The currents were sampled at 0.05 ms/point and filtered at 1 kHz, through an 8-pole Bessel filter. Single-channel data analyses were performed with pClamp, TIPS, and custom software.

RESULTS

The entire protein-coding sequence of rabbit skeletal muscle RyR cDNA was cloned into pRRS11 expression vector (Takeshima et al., 1989; Penner et al., 1989). A deletion mutant was derived after digesting pRRS11 with *SalI* (nt 546) and *XhoI* (nt 12018) and religating the plasmid (Fig. 1

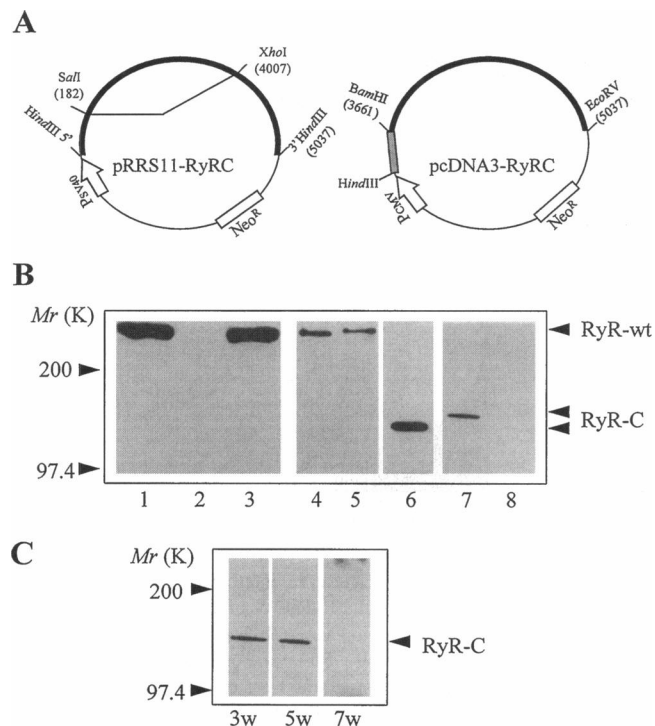


FIGURE 1 Expression of full-length and carboxyl-terminal RyR proteins in CHO cells. (A) Schematic representation of expression plasmids for RyR-C. pRRS11-RyRC lacks the RyR cDNA sequence from nt 547 (*SalI*) through nt 12018 (*XhoI*), and encodes an RyR protein that lacks 3824 residues (a.a. 183 through 4006) in the foot region (left). pcDNA3-RyRC contains cDNA encoding the C-terminal 1377 residues (a.a. 3661 to 5037) (right). The cross-hatched bar in pcDNA3-RyRC represents a 45-bp oligonucleotide containing the following sequence: 5'-*HindIII*-KOZAK-6xHis-*BamHI*-3' (see Materials and Methods). (B) Immunoblot analysis of RyR proteins expressed in CHO cells. RyR proteins were immunoprecipitated from cell lysate and blotted with RR2 antibody against rabbit skeletal muscle RyR. CHO cells transfected with pRRS11 using electroporation (lane 4) and lipofectamine (lane 5) express a high-molecular-mass protein of ~560 kDa that is identical to the native RyR in rabbit skeletal muscle (lane 1) and to the RyR stably expressed in CHO cells (lane 3). Cells transfected with pRRS11-RyRC (lane 6) and pcDNA3-RyRC (lane 7) express the truncated RyR proteins, which can be recognized by RR2. Untransfected cells (lane 2) and cells transfected with pcDNA3 alone (lane 8) do not contain detectable amounts of RyR proteins. (C) Time course of expression of RyR-C protein. The levels of RyR-C expression in CHO cells declined ~7 weeks (lane 3) after transfection with pcDNA3-RyRC.

A, left). This mutant plasmid (pRRS11-RyRC) contains cDNA encoding the first amino-terminal 182 and carboxyl-terminal 1030 amino acids, which includes the putative transmembrane segments of RyR. An alternative expression plasmid (pcDNA3-RyRC) was constructed by cloning the 4.2-kb RyR cDNA encoding the carboxyl-terminal 1377 amino acids into pcDNA3 expression vector, followed by the introduction of a 45-bp oligonucleotide containing the consensus KOZAK sequence (Fig. 1 A, right).

CHO cells were transfected with the full-length expression plasmid (pRRS11) or with the truncation plasmids (pRRS11-RyRC or pcDNA3-RyRC) and cultured in the presence of G418. The expression of protein products was assayed by immunoblotting analysis (Fig. 1, B and C). Cells

transfected with pRRS11 expressed a high- M_r protein (RyR-wt), identical to RyR from skeletal muscle SR, both of which were recognized by monoclonal antibody (RR2) against rabbit skeletal muscle RyR (Fig. 1 B). Transfection with pRRS11-RyRC resulted in a protein product of ~130 kDa, and pcDNA3-RyRC resulted in a protein product of ~150 kDa, both of which were recognized by RR2 (Fig. 1 B). The expression of RyR-C in CHO cells was maintained for at least 5 weeks, after which the protein levels decreased (Fig. 1 C). No protein was recognized by RR2 in untransfected CHO cells, or in those transfected with pcDNA3 alone, suggesting that CHO cells do not contain any detectable amount of endogenous RyR protein.

The Ca^{2+} release channel functions of the expressed RyR-wt and RyR-C were measured after reconstituting microsomal membrane vesicles from transfected cells into lipid bilayer membranes, using cesium gluconate as the current-carrying ion in the recording solution (Fig. 2). The use of Cs as current carrier allows buffering of the free $[\text{Ca}^{2+}]$ to any desired level. In addition, Cs eliminates most of the potassium channel activities present in the microsome membrane vesicles, and the large anion gluconate does not permeate through the endogenous chloride channel(s) present in the endoplasmic reticulum membranes of CHO cells.

Both RyR-wt and RyR-C channels displayed fast kinetics of transition between open and closed states (Fig. 2 A), and both channels were sensitive to modification by ryanodine (Fig. 2 B), which are characteristic features of the native Ca^{2+} release channels (Rousseau et al., 1987; Ma and Zhao, 1994; Ma et al., 1995). One of the noticeable differences between RyR-wt and RyR-C is that the RyR-C channel gates frequently in the presence of ryanodine. Open time histogram analyses revealed two time constants, $\tau_{o1} = \sim 0.4$ ms and $\tau_{o2} = \sim 3.0$ ms, associated with both RyR-native and expressed RyR-wt channels (Fig. 2 C). The gating kinetics of the RyR-C channel were different from those of RyR-wt in that the open events with longer durations (τ_{o2}) occurred more frequently ($y_{o2}/(y_{o1} + y_{o2}) = 0.18$, RyR-wt; $y_{o2}/(y_{o1} + y_{o2}) = 0.37$, RyR-C, at +50 mV) (Fig. 2 C).

Under symmetrical ionic conditions of 200 mM Cs-gluconate, the RyR-native and RyR-wt channels conducted Cs ions equally well in both inward (–50 mV) and outward (+50 mV) directions (Fig. 2 A, left and middle), such that the current-voltage relationship was linear over the voltage range from –80 to +80 mV (Ma et al., 1997). However, the RyR-C channel exhibited significant inward rectification in that the amplitude of the outward current (cytoplasm→SR lumen) was smaller than that of the inward current (SR lumen→cytoplasm) (Fig. 2 A, right). At +50 mV, the mean current amplitude was 20.24 ± 0.69 pA for RyR-wt ($n = 13$), and 14.64 ± 0.95 pA for RyR-C ($n = 8$), whereas at –50 mV, the mean current amplitudes for RyR-wt and RyR-C were similar (-19.24 ± 0.91 pA, RyR-wt, $n = 12$; -19.57 ± 0.74 pA, RyR-C, $n = 7$) (see also Fig. 3 A). The RyR-C channel had an inward conductance of 407 ± 16.0

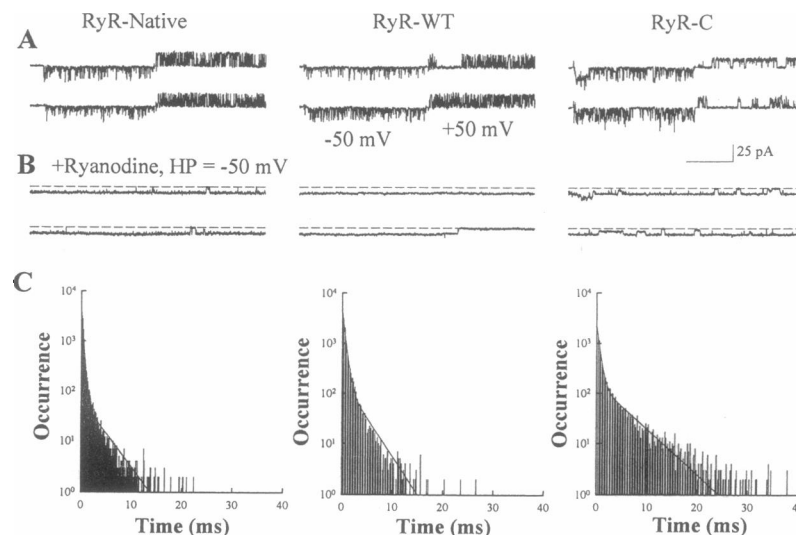


FIGURE 2 Reconstitution of native RyR, RyR-wt, and RyR-C channel activities in lipid bilayer membranes. (A) Representative single-channel currents through the native Ca^{2+} -release channel from rabbit skeletal muscle (left), expressed RyR-wt channel (middle), and RyR-C channel (right) were measured with a pulse protocol of $-50 \rightarrow +50$ mV. Inward deflections represent Cs ions moving from SR lumen to cytoplasm. (B) The same channels after the addition of 5 μM ryanodine changed their kinetics of gating from fast to slow, and reduced their conductance by $\sim 50\%$. The calibration bar corresponds to 100 ms for the control channels (A) and 200 ms for the ryanodine-modified channels (B). (C) Open time histograms were calculated at test pulses of -50 mV for the native channel (left) and at $+50$ mV for the expressed RyR-wt (middle) and RyR-C channels (right). The data were combined from a total of 12 experiments with the native channel (total open events (n) = 10,382), 13 experiments with the RyR-wt channel (n = 8860), and 10 experiments with the RyR-C channel (n = 6760). Solid lines are the best fits according to $y = y_{o1}/\tau_{o1}\exp(-t/\tau_{o1}) + y_{o2}/\tau_{o2}\exp(-t/\tau_{o2})$, with the following parameters: $y_{o1} = 1515$, $\tau_{o1} = 0.31$ ms, $y_{o2} = 214$, $\tau_{o2} = 3.29$ ms (left); $y_{o1} = 2347$, $\tau_{o1} = 0.49$ ms, $y_{o2} = 512$, $\tau_{o2} = 2.90$ ms (middle); $y_{o1} = 1240$, $\tau_{o1} = 0.55$ ms, $y_{o2} = 734$, $\tau_{o2} = 4.85$ ms (right).

pS (0 to -80 mV; Fig. 3 B), which is similar to that of the RyR-wt channel (Ma et al., 1997), but the outward conductance through the RyR-C channel was significantly smaller ($G = 332 \pm 18.9$ pS; Fig. 3 B). Whereas the results shown for RyR-C are taken from experiments done with CHO cells expressing pRRS11-RyRC, similar results were also obtained from cells expressing pcDNA3-RyRC ($n = 24$, data not shown).

Similar to the RyR-native and RyR-wt channels, opening of the RyR-C channels absolutely required the presence of micromolar concentrations of Ca^{2+} in the cytoplasmic solution (Fig. 4 A, left). Chelating the free $[\text{Ca}^{2+}]$ from 220 μM to <40 nM with EGTA caused the RyR-C channel to

close completely (Fig. 4 A, middle, $n = 4$). The effect of EGTA was reversible, as subsequent addition of CaCl_2 to the cytoplasmic solution restored channel opening (Fig. 4 A, right, $n = 3$). The dose-response relationship of channel opening probability as a function of cytoplasmic Ca was illustrated in Table 1. Activation of the RyR-wt channel had a dissociation constant (K_d) for cytoplasmic $[\text{Ca}]$ of ~ 0.25 μM (Ma et al., 1997), whereas activation of the RyR-C channel had a K_d of ~ 2 – 20 μM (Table 1). Therefore it appears that the RyR-C proteins retain the binding site(s) for cytoplasmic Ca that participate in Ca-dependent activation of the Ca release channel, and this activation required higher cytoplasmic $[\text{Ca}]$.

FIGURE 3 Current amplitude histogram and I - V relationship of the RyR-C channel. (A) The all-point current amplitude histogram was generated with 16 consecutive episodes of single-channel currents obtained with a similar pulse protocol given in Fig. 2 A, in a bilayer containing a RyR-C channel. The solid lines represent the best fit with Gaussian distribution functions, with the following parameters (mean \pm SD): $I_{-50} = -18.7 \pm 1.48$ pA, and $I_{+50} = +13.5 \pm 1.00$ pA. (B) Current-voltage relationship of the RyR-C channel. The channel had an inward conductance of 407 ± 16.0 pS (0 to -80 mV, —) and an outward conductance of 332 ± 18.9 pS (0 to $+80$ mV, ---).

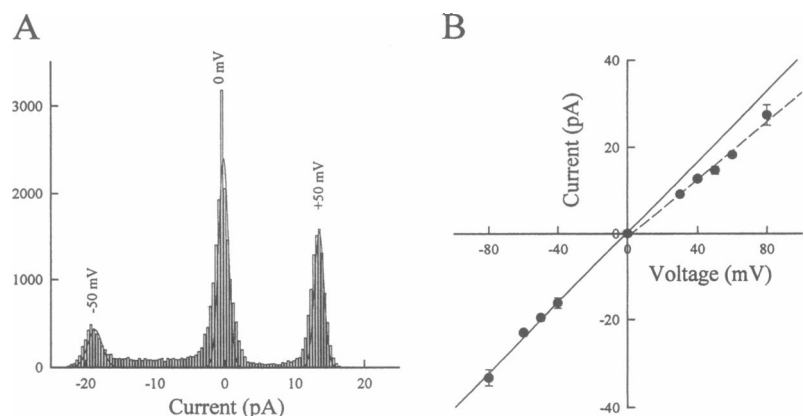
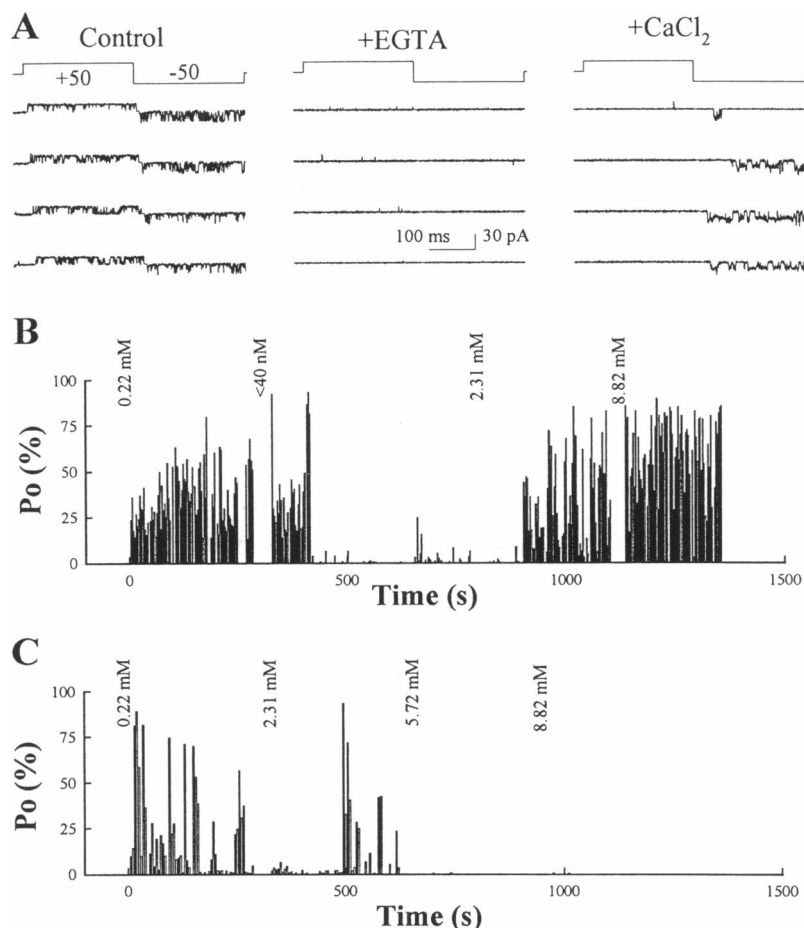


FIGURE 4 Ca^{2+} -dependent activation and inactivation of RyR-wt and RyR-C channels. (A) Consecutive single-channel currents through a RyR-C channel were obtained with test pulses of $+50 \rightarrow -50$ mV, in the presence of $220 \mu\text{M}$ free $[\text{Ca}^{2+}]$ in the *cis* solution (Control), after addition of 10 mM EGTA to the *cis* solution (free $[\text{Ca}^{2+}] < 40 \text{ nM}$) (+EGTA), and after addition of 20 mM CaCl_2 to the *cis* solution (free $[\text{Ca}^{2+}] = 2.31 \text{ mM}$) (+ CaCl_2). The pH in the solution was adjusted to 7.5 with calibrated amounts of Tris-base. (B) Open probabilities (P_o) of RyR-C channel at -50 mV were calculated from the same experiment as shown in A, and plotted as a function of time, after sequential additions of EGTA and CaCl_2 to the *cis* solution. The numbers indicated by the arrows represent the amount of free $[\text{Ca}^{2+}]$ (determined with a Ca^{2+} -sensitive electrode) present in the *cis* solution. The delay in channel closure in response to EGTA application is due to the diffusion-limited process. (C) Similar titration experiments were performed with the RyR-wt channel, with the addition of CaCl_2 to the *cis* solution. The diary plots show that the RyR-wt channel closes at high $[\text{Ca}^{2+}]$, whereas the RyR-C channel does not.



Striking differences between RyR-wt and RyR-C channels were observed at high Ca^{2+} concentrations. The RyR-wt channel, similar to the native Ca^{2+} release channel, was sensitive to inhibition by cytoplasmic Ca^{2+} (Fig. 4 C, $n = 6$) (Ma and Zhao, 1994; Ma et al., 1997). In contrast, the RyR-C channel failed to close at free cytoplasmic $[\text{Ca}^{2+}]$ up to 8.82 mM (Fig. 4 B, $n = 5$). These results suggest that the low-affinity binding site(s) responsible for Ca^{2+} -dependent inactivation were lost in the truncated RyR protein. This is consistent with the hypothesis that there are

two independent sites for Ca^{2+} activation and inactivation in the skeletal muscle RyR protein (Chu et al., 1993; Laver et al., 1995).

In $\sim 20\%$ of the experiments with RyR-C, a large-conductance channel with slow kinetics of gating was measured (Fig. 5 A; $n = 22/104$). This large current, with an amplitude of up to $+70 \text{ pA}$ at $+80 \text{ mV}$, was associated with the expression of RyR-C proteins, because no such currents were measured in untransfected CHO cells, or in cells transfected with pcDNA3 alone. There appeared to be a close association between the normal fast-gating RyR-C Ca^{2+} release channel (Figs. 2 and 4) and the large slow-gating channel (Fig. 5), because the appearance of these large conductance channels was almost always accompanied by the normal open events of RyR-C (Fig. 5 A, *top trace*). Although the amplitude of the large-conductance channel was reduced with the addition of EGTA, it could not be inhibited completely (Fig. 5 B, $n = 3$). Ryanodine did not produce detectable changes in conductance states or gating kinetics of these large-conductance channels (within 15–30 min after the addition of $5 \mu\text{M}$ ryanodine to both *cis* and *trans* solutions; $n = 3$). We do not clearly understand the mechanism behind this large-conductance channel. One possible explanation is that these channels reflect a defective oligomerization state of the RyR-C protein.

TABLE 1 Ca -dependent activation of RyR-wt and RyR-C channels

$[\text{Ca}]_i$	RyR-wt	RyR-C
8.82 mM	0.015 ± 0.005 ($n = 6$)	0.220 ± 0.034 ($n = 6$)
2.31 mM	0.090 ± 0.013 ($n = 14$)	0.196 ± 0.042 ($n = 5$)
$220 \mu\text{M}$	0.121 ± 0.044 ($n = 19$)	0.201 ± 0.036 ($n = 12$)
$30 \mu\text{M}$	0.129 ± 0.028 ($n = 5$)	0.095 ± 0.020 ($n = 3$)
$0.25 \mu\text{M}$	0.062 ± 0.010 ($n = 8$)	0.074 ± 0.033 ($n = 2$)
$0.08 \mu\text{M}$	0.013 ± 0.002 ($n = 5$)	0.008 ± 0.003 ($n = 4$)
$0.02 \mu\text{M}$	0.002 ± 0.001 ($n = 6$)	0.000 ± 0.000 ($n = 5$)

The listed numbers (mean \pm SE) were open probabilities of the single RyR-wt and RyR-C channels calculated at $+50 \text{ mV}$ test potential. $[\text{Ca}]_i$, Concentration of free Ca in the cytoplasmic solution; n , the number of experiments.

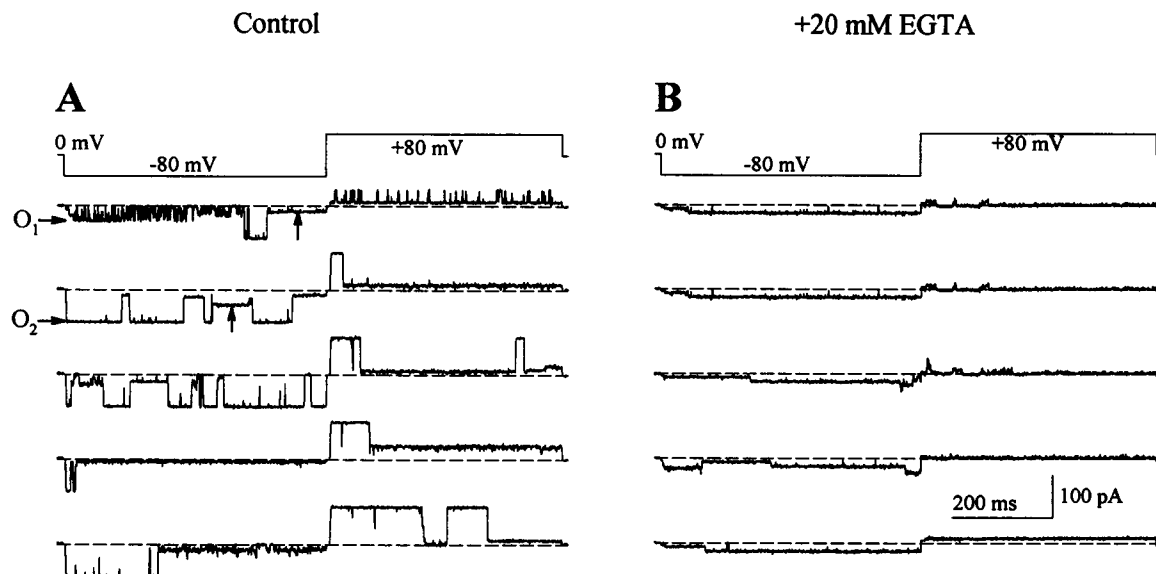


FIGURE 5 Large-conductance channel associated with expression of RyR-C in CHO cells. Consecutive single-channel episodes were recorded after fusion of microsomal membrane vesicles containing the RyR-C proteins to the lipid bilayer membrane. (A) In the presence of $220 \mu\text{M}$ $[\text{Ca}^{2+}]$ in the *cis* solution, both normal fast gating events (labeled O_1) and large slow open events (labeled O_2) were measured. The bilayer contained at least two channels with conductance states O_1 and O_2 , respectively. The intermediate conductance levels (indicated by the arrows) probably reflect the subconductance states of the O_2 channel. The largest current amplitudes were $\sim 70 \text{ pA}$ at $+80 \text{ mV}$. (B) Addition of 20 mM EGTA to the *cis* solution completely inhibited the O_1 channel, but only partially inhibited the O_2 channel. In the presence of EGTA, the O_2 channel was reduced to the lower conductance states. The data were representative of 22 of 104 experiments with the RyR-C channels.

DISCUSSION

Our results suggest that the carboxyl-terminal portion ($\sim 20\%$) of the skeletal muscle RyR contains structures sufficient to form a functional Ca^{2+} release channel, which is sensitive to modulation by ryanodine. This truncated Ca^{2+} release channel retains its normal conduction properties at least when moving Cs ions from SR lumen to cytoplasm (Fig. 2 A), and its sensitivity to activation by micromolar concentrations of cytoplasmic Ca^{2+} (Fig. 3 A). Within the RyR-C protein there are several potential Ca^{2+} -binding sites (a.a. 4253–4264, 4407–4416, 4489–4499) that could presumably contribute to the Ca^{2+} -dependent activation of the channel (Takeshima et al., 1989). Several differences between RyR-wt and RyR-C are identified in the present study. First, the RyR-C channel in the presence of ryanodine seems to undergo frequent transitions between open and closed states; second, the RyR-C channel exhibits inward rectification when conducting cesium ions; and third, the RyR-C channel lacks apparent Ca^{2+} -dependent inactivation (Table 2). These results point out the importance of the foot region of RyR in the function of the Ca^{2+} release channel; in particular, our study suggests that different Ca^{2+} -binding sites may be responsible for activation and inactivation properties of the release channel by cytoplasmic Ca^{2+} .

The asymmetrical conductance of the RyR-C channel (Fig. 3 B) and the lack of Ca^{2+} -dependent inactivation (Fig. 4 B) suggest the importance of the amino-terminal cytoplasmic region or a portion thereof in the conduction property

and Ca^{2+} -dependent regulation of the Ca^{2+} release channel. Results from our recent study support this idea, in that deletion of a negatively charged domain in the amino-terminal region causes the resulting channel to rectify, as does the RyR-C channel (Bhat et al., 1997). Thus a disturbance in membrane surface potential caused by the lack of a charged domain may be responsible for the altered conduction of the truncated Ca^{2+} release channel. Within the foot structure of skeletal RyR, there is a sequence of 18 consecutive glutamates (a.a. 1873 to 1890, rabbit RyR) that may form a potential low-affinity Ca^{2+} -binding site, as initially suggested by Zorzato and colleagues (Zorzato et al., 1990). By using peptide overlay analysis, a Ca^{2+} -binding domain has been shown to reside between residues 1861 and 2094 of the skeletal muscle RyR (Chen and MacLennan, 1994). Interestingly, the amino acid sequences of skeletal and cardiac RyR diverge in this region (D3 region, a.a. 1872–1923 in skeletal and 1852–1890 in cardiac RyR), which contains negative charges in the skeletal RyR but not

TABLE 2 Single-channel properties of RyR-wt and RyR-C

	RyR-wt	RyR-C
Open lifetimes	$\tau_{o1} = 0.49 \text{ ms}$ $\tau_{o2} = 2.90 \text{ ms}$	$\tau_{o1} = 0.55 \text{ ms}$ $\tau_{o2} = 4.85 \text{ ms}$
Inward conductance	$406 \pm 4.0 \text{ pS}$	$407 \pm 16.0 \text{ pS}$
Outward conductance	$406 \pm 4.0 \text{ pS}$	$332 \pm 18.9 \text{ pS}$
Ryanodine effect	Yes	Yes
Ca activation	Yes	Yes
Ca inactivation	Yes	No

in the cardiac counterpart (Sorrentino and Volpe, 1993; Takeshima, 1993). It is well known that the cardiac RyR channels, unlike the skeletal subtypes, are less susceptible to inhibition by cytoplasmic Ca^{2+} , in that at least 10-fold more $[\text{Ca}^{2+}]$ is required to inactivate the cardiac channel (Chu et al., 1993; Laver et al., 1995). The fact that the skeletal RyR channels lacking the D3 region ($\Delta\text{D3-RyR}$; Bhat et al., 1997) and RyR-C do not exhibit apparent Ca^{2+} -dependent inactivation suggests that the D3 region in the foot region contains the putative binding site(s) for Ca^{2+} -dependent inactivation of the skeletal muscle Ca^{2+} release channel.

Both skeletal and cardiac subtypes of RyR contain stretches of negatively charged amino acids at the carboxyl-terminal end (the loops joining transmembrane segments M1 and M2, and M3 and M4), which is predicted to extend into the luminal side of the SR membrane (Takeshima et al., 1989). These negatively charged residues could, in principle, concentrate the permeating cations in the pore region of the Ca^{2+} release channel and facilitate the movement of cations from the SR lumen to the cytoplasm, thus leading to the asymmetrical feature of the current-voltage relationship, as has been shown with the native cardiac Ca^{2+} release channel (Tu et al., 1994).

In summary, this study demonstrates that the carboxyl-terminal portion of the skeletal muscle RyR is sufficient to form a functional Ca^{2+} release channel. Our data are consistent with the hypothesis that RyR has two roles in E-C coupling of skeletal muscle, as a signal transducer and as a mediator of intracellular Ca^{2+} release. Although RyR is the major intracellular Ca^{2+} release channel in striated muscles, it is also expressed in a variety of tissues, including smooth muscle (Herrmann-Frank et al., 1991) and brain (McPherson et al., 1991), where it participates in the regulation of intracellular Ca^{2+} homeostasis. RyR is also related to inositol 1,4,5-trisphosphate receptor (IP_3R), which functions as an intracellular Ca^{2+} release channel in most cell types. The structural similarity between RyR and IP_3R is striking, especially in the carboxyl-terminal hydrophobic region, where these proteins share >30% sequence identity (Taylor and Traynor, 1995). Thus our finding that the pore-forming region of the skeletal muscle Ca^{2+} release channel resides in the carboxyl-terminal portion of RyR may help in understanding not only the mechanism of E-C coupling in striated muscles, but also the regulation of intracellular Ca^{2+} homeostasis in general.

We thank Drs. Junxia Xie and Mitchell L. Drumm for initial help with the expression and mutagenesis experiments, and Drs. S. W. Jones and A. Scarpa for reading the manuscript.

This work was supported by the National Institutes of Health, American Heart Association, Muscular Dystrophy Association, and by the Pilot Project of the Howard Hughes Medical Institute (JM).

REFERENCES

- Bhat, M. B., J. Zhao, S. Hayek, E. C. Freeman, H. Takeshima, and J. Ma. 1997. Deletion of a.a. 1641–2437 from the foot region of skeletal muscle ryanodine receptor alters conduction properties of the calcium release channel. *Biophys. J.* 73:1320–1328.
- Block, B. A., T. Imagawa, K. P. Campbell, and C. Franzini-Armstrong. 1988. Structural evidence for a direct interaction between the molecular components of the transverse tubule/sarcoplasmic reticulum junction in skeletal muscle. *J. Cell Biol.* 107:2587–2600.
- Brillantes, A. B., K. Ondrias, A. Scott, E. Koblinsky, E. Ondriasova, M. C. Moschella, T. Jayaraman, M. Landers, B. E. Ehrlich, and A. R. Marks. 1994. Stabilization of calcium release channel (ryanodine receptor) function by FK506-binding protein. *Cell.* 77:513–523.
- Callaway, C., A. Seryshev, J. P. Wang, K. J. Slavik, D. H. Needleman, C. Cantu, Y. Wu, T. Jayaraman, A. R. Marks, and S. L. Hamilton. 1994. Localization of the high and low affinity [^3H]-ryanodine binding sites on the skeletal muscle Ca release channel. *J. Biol. Chem.* 269: 15876–15884.
- Chen, S. R. W., and D. H. MacLennan. 1994. Identification of calmodulin-, Ca- and ruthenium red-binding domains in the Ca release channel (ryanodine receptor) of rabbit skeletal muscle sarcoplasmic reticulum. *J. Biol. Chem.* 269:22698–22704.
- Chu, A., M. Fill, E. Stefani, and M. L. Entman. 1993. Cytoplasmic Ca does not inhibit the cardiac muscle sarcoplasmic reticulum ryanodine receptor Ca channel, although Ca-induced Ca release is observed in native vesicles. *J. Membr. Biol.* 135:49–59.
- Coronado, R., J. Morrisette, M. Sukhareva, and D. M. Vaughan. 1994. Structure and function of ryanodine receptors. *Am. J. Physiol.* 266: C1485–C1504.
- Fleischer, S., and M. Inui. 1989. Biochemistry and biophysics of excitation-contraction coupling. *Annu. Rev. Biophys. Chem.* 18: 333–364.
- Franzini-Armstrong, C., and A. O. Jorgensen. 1994. Structure and development of E-C coupling units in skeletal muscle. *Annu. Rev. Physiol.* 56:509–534.
- Herrmann-Frank, A., E. Darling, and G. Meissner. 1991. Functional characterization of the Ca^{2+} -gated Ca^{2+} release channel of vascular smooth muscle sarcoplasmic reticulum. *Pflügers Arch.* 418:353–359.
- Imagawa, T., J. S. Smith, R. Coronado, and K. P. Campbell. 1987. Purified ryanodine receptor from muscle sarcoplasmic reticulum is the Ca^{2+} -permeable pore of the calcium release channel. *J. Biol. Chem.* 262: 16636–16643.
- Lai, F. A., H. Erickson, E. Rousseau, Q. Y. Liu, and G. Meissner. 1988. Purification and reconstitution of the calcium release channel from skeletal muscle. *Nature.* 331:315–319.
- Lai, F. A., M. Misra, L. Xu, H. A. Smith, and G. Meissner. 1989. The ryanodine receptor-Ca release channel complex of skeletal muscle sarcoplasmic reticulum. Evidence for a cooperatively coupled, negatively charged homotetramer. *J. Biol. Chem.* 264:16776–16785.
- Laver, D. R., L. D. Roden, G. P. Ahern, K. R. Eager, P. R. Junankar, and A. F. Dulhunty. 1995. Cytoplasmic Ca inhibits the ryanodine receptor from cardiac muscle. *J. Membr. Biol.* 147:7–22.
- Ma, J., M. B. Bhat, and J. Y. Zhao. 1995. Rectification of skeletal muscle ryanodine receptor mediated by FK506 binding protein. *Biophys. J.* 69:2398–2404.
- Ma, J., M. Fill, M. Knudson, K. P. Campbell, and R. Coronado. 1988. Ryanodine receptor is a gap junction-type channel. *Science.* 242: 99–102.
- Ma, J., and J. Y. Zhao. 1994. Highly cooperative and hysteretic response of the skeletal muscle ryanodine receptor to changes in proton concentrations. *Biophys. J.* 67:626–633.
- McPherson, P. S., and K. P. Campbell. 1993. The ryanodine receptor/ Ca^{2+} release channel. *J. Biol. Chem.* 268:13765–13768.
- McPherson, P. S., Y.-K. Kim, H. Valdivia, C. M. Knudson, H. Takekura, C. Franzini-Armstrong, R. Coronado, and K. P. Campbell. 1991. The brain ryanodine receptor: a caffeine-sensitive calcium release channel. *Neuron.* 7:17–25.
- Meissner, G. 1994. Ryanodine receptor/Ca release channels and their regulation by endogenous effectors. *Annu. Rev. Physiol.* 56:485–508.
- Nakai, J., T. Imagawa, M. Hakamata, H. Shigekawa, H. Takeshima, and S. Numa. 1990. Primary structure and functional expression from cDNA of the cardiac ryanodine receptor/calcium release channel. *FEBS Lett.* 271:169–177.

- Otsu, K., H. F. Willard, V. K. Khanna, F. Zorzato, N. M. Green, and D. H. MacLennan. 1990. Molecular cloning of cDNA encoding the Ca release channel (ryanodine receptor) of rabbit cardiac muscle sarcoplasmic reticulum. *J. Biol. Chem.* 265:13472–13483.
- Penner, R., E. Neher, H. Takeshima, S. Nishimura, and S. Numa. 1989. Functional expression of the calcium release channel from skeletal muscle ryanodine receptor cDNA. *FEBS Lett.* 259:217–221.
- Rios, E., J. Ma, and A. Gonzalez. 1991. The mechanical hypothesis of excitation-contraction (E-C) coupling in skeletal muscle. *J. Muscle Res. Cell. Motil.* 12:127–135.
- Rios, E., G. Pizarro, and E. Stefani. 1992. Charge movement and the nature of signal transduction in skeletal muscle excitation-contraction coupling. *Annu. Rev. Physiol.* 54:109–133.
- Rousseau, E., J. S. Smith, and G. Meissner. 1987. Ryanodine modifies conductance and gating behavior of single Ca release channel. *Am. J. Physiol.* 253:364–368.
- Smith, J. S., R. Coronado, and G. Meissner. 1985. Sarcoplasmic reticulum contains adenine nucleotide-activated calcium channels. *Nature.* 316:446–449.
- Smith, J. S., T. Imagawa, J. Ma, M. Fill, K. P. Campbell, and R. Coronado. 1988. Purified ryanodine receptor from rabbit skeletal muscle is the calcium-release channel of sarcoplasmic reticulum. *J. Gen. Physiol.* 92:1–26.
- Sorrentino, V., and P. Volpe. 1993. Ryanodine receptors: how many, where and why? *Trends Pharmacol. Sci.* 14:98–103.
- Sutko, J. L., and J. A. Airey. 1996. Ryanodine receptor Ca^{2+} release channels: does diversity in form equal diversity in function? *Physiol. Rev.* 76:1027–1071.
- Takeshima, H. 1993. Primary structure and expression from cDNAs of the ryanodine receptor. *Ann. N.Y. Acad. Sci.* 707:165–177.
- Takeshima, H., S. Nishimura, T. Matsumoto, H. Ishida, K. Kangawa, N. Minamino, H. Matsuo, M. Ueda, M. Hanaoka, T. Hirose, and S. Numa. 1989. Primary structure and expression from complementary DNA of skeletal muscle ryanodine receptor. *Nature.* 339:439–445.
- Takeshima, H., S. Nishimura, M. Nishi, M. Ikeda, and T. Sugimoto. 1993. A brain-specific transcript from the 3'-terminal region of the skeletal muscle ryanodine receptor region. *FEBS. Lett.* 322:105–110.
- Taylor, C. W., and D. Traynor. 1995. Calcium and inositol trisphosphate receptors. *J. Membr. Biol.* 145:109–118.
- Tu, Q., P. Velez, M. Cortes-Gutierrez, and M. Fill. 1994. Surface charge potentiates conduction through the cardiac ryanodine receptor channel. *J. Gen. Physiol.* 103:853–867.
- Wagenknecht, T., R. Grassucci, J. Frank, A. Saito, M. Inui, and S. Fleischer. 1989. Three dimensional architecture of the calcium channel/foot structure of sarcoplasmic reticulum. *Nature.* 338:167–170.
- Witcher, D. R., P. S. McPherson, S. D. Kahl, T. Lewis, P. Bentley, M. J. Mullinix, J. D. Windass, and K. P. Campbell. 1994. Photoaffinity labeling of the ryanodine receptor/Ca release channel with an azido derivative of ryanodine. *J. Biol. Chem.* 269:13076–13079.
- Zorzato, F., J. Fujii, K. Otsu, N. M. Green, F. A. Lai, G. Meissner, and D. H. MacLennan. 1990. Molecular cloning of cDNA encoding human rabbit forms of the Ca release channel (ryanodine receptor) of skeletal muscle sarcoplasmic reticulum. *J. Biol. Chem.* 265:2244–2256.